cerebral vascular disease 4

world federation of neurology
11th salzburg conference

editors
j.s. meyer, h. lechner,
m. reivich and e.o. ott

CEREBRAL VASCULAR DISEASE 4

Proceedings of the World Federation of Neurology 11th International Salzburg Conference, September 23-25, 1982

Editors:
J.S. MEYER, H. LECHNER, M. REIVICH and E.O. OTT

1983

Excerpta Medica, Amsterdam-Oxford-Princeton

International Congress Series No. 616

ISBN Excerpta Medica 90 219 0616 3
ISBN Elsevier Science Publishing Co. 0 444 90314 3

Library of Congress Cataloging in Publication Data

International Salzburg Conference (11th : 1982)
Cerebral vascular disease, 4.

(International congress series ; no. 616)
Includes bibliographical references and index.
1. Cerebrovascular disease--Congresses. I. Meyer, John Stirling. II. World Federation of Neurology. III. Title. IV. Series.
RC388.5.I514 1982 616.8'1 83-5639
ISBN 0-444-90314-3 (Elsevier)

Publisher:
Excerpta Medica
305 Keizersgracht
P.O. Box 1125
1000 BC Amsterdam

Sole Distributors for the USA and Canada:
Elsevier Science Publishing Co. Inc.
52 Vanderbilt Avenue
New York, N.Y. 10017

Printed in The Netherlands by Casparie, Amsterdam

INTERNATIONAL SALZBURG CONFERENCE
ON CEREBRAL VASCULAR DISEASE

founded by

H. BERTHA, O. EICHHORN, H. LECHNER

organized by

FEDERATION MONDIALE DE NEUROLOGIE
WORLD FEDERATION OF NEUROLOGY

Research Group on Cerebrovascular Disease

GENERAL COMMENTS

Fifty-three papers were selected for presentation by 231 listed authors and co-authors at the Salzburg Conference. Authors were from Austria, Canada, Denmark, UK, Finland, France, Holland, India, Italy, Japan, Norway, Peru, USA, West Germany.

The topics included: In vivo measurements of cerebral blood flow and metabolism, Aging and risk factors influencing cerebral blood flow and incidence of stroke, Platelet aggregation in patients with transient ischemic attacks (TIA) and reversible ischemic neurological deficits (RIND), Autoregulation of cerebral blood flow, Neurogenic hyper- and hypo-tension in vertebral basilar arterial ischemia, Cerebral embolism, Nuclear magnetic imaging in cerebrovascular disease, Multi-dimensional analysis for predicting prognosis in stroke, Ultrasonic scanning and digital subtraction, Intravenous angiography in cerebrovascular disease, Anti-platelet aggregation, Treatment in cerebrovascular disease, Hemodilution as a treatment for stroke, Calcium (Ca^{2+}) entry blockers in cerebral infarction, International extracranial-intracranial (EC/IC) by-pass study, Total microsurgical excision of cerebral AVMs, Role of aneurysmal size to rupture of aneurysms, CT scans, Assessment of neurologically silent strokes and multi-infarct dementia (MID), Cerebral blood flow in dementia, Evidence for neuroplasticity after experimental infarction, and New concepts of cerebrovascular mechanisms in migraine.

The consensus was that this was a valuable meeting with an excellent opportunity to review "state of the art" developments in methodology, exchange new information and participate in the ample time provided for discussion. The meeting was opened by Dr. Helmut Lechner (Graz, Austria), the organizing secretary and by the Chairman, Dr. John Marshall (UK).

CONTENTS

II. NEUROIMAGING TECHNIQUES

III. CRITICAL EVALUATION OF THERAPEUTIC APPROACHES

BERTHA MEMORIAL LECTURE

MEASUREMENT OF LOCAL CEREBRAL GLUCOSE UTILIZATION: ITS USE IN LOCALIZING NORMAL AND ABNORMAL FUNCTIONAL ACTIVITIES IN THE NERVOUS SYSTEM

L. Sokoloff

Laboratory of Cerebral Metabolism, NIMH, Bethesda, MD 20205. Bertha Memorial Lecture, International Salzburg Conference on Cerebrovascular Disease, September 1982

The brain is a complex, heterogeneous organ composed of an almost infinite number of structural and functional components with widely different and independently regulated levels of functional and metabolic activities. In most tissues that do physico-chemical work, there is a close relationship between the level of functional activity and the rate of energy metabolism. Under most normal circumstances glucose is the almost exclusive substrate for the brain's energy metabolism, and its rate of utilization is a reasonable measure of the energy metabolism of cerebral tissue. A method has been developed for the quantitative determination of the rates of glucose utilization simultaneously in all the structural and functional components of the nervous system. The method is applicable to normal conscious animals as well as those in experimentally altered states of cerebral activity. The results of a number of studies with this method have demonstrated that there is in the nervous system a close coupling between the level of local functional activity and the local rate of energy metabolism (9).

The method utilizes tracer doses of radioactive 2-deoxy-D-glucose to trace glucose metabolism. This analogue of glucose shares and competes with glucose for the carrier that transports them bi-directionally across the blood-brain barrier. It also competes with glucose for hexokinase, the enzyme that phosphorylates both to their respective hexose-6-phosphates. Once formed, glucose-6-phosphate is rapidly converted to fructose-6-phosphate and metabolized further ultimately to CO_2 and H_2O. In contrast, 2-deoxyglucose-6-phosphate, which lacks a hydroxyl group on the second carbon position, cannot be converted to fructose-6-phosphate. It is also a poor substrate for glucose-6-phosphate dehydrogenase and other enzymes in brain that act upon glucose-6-phosphate. It is hydrolyzed very slowly because of very low deoxyglucose-6-phosphatase activity in brain. Deoxyglucose-6-phosphate, once formed, is, therefore, essentially trapped in the cells, at least for a reasonable amount of time, and the amount accumulated is a measure of the amount of deoxyglucose that has been phosphorylated. The amount of deoxyglucose phosphorylated

is in turn related to the amount of glucose phosphorylated over the same interval of time, depending on the relative concentrations of the competing substrates for hexokinase and the Michaelis-Menten constants of the enzyme for the two substrates. In a steady state, the net rate of glucose phosphorylation by hexokinase is equal to the rate of glucose utilization.

A kinetic model based on these biochemical properties of 2-deoxyglucose and glucose in brain has been constructed and mathematically analyzed to derive an operational equation that permits the calculation of the local rates of cerebral glucose utilization from measurable variables (Fig. 1) (12).

The equation requires the measurement of the time courses of the arterial plasma deoxyglucose and glucose concentrations for a period of 30-45 minutes following an intravenous pulse of [^{14}C] deoxyglucose and the final tissue concentrations of [^{14}C]. It also requires values for the rate constants of the transport of deoxyglucose across the blood-brain barrier and its phosphorylation by hexokinase and also a combination of six constants, the so-called "lumped constant", which is a combination of the ratios of the K_m and V_{max} values of hexokinase for deoxyglucose and glucose and also the ratio of their distribution spaces in the tissue. These constants have been determined separately in other groups of animals, and they can then be used in the equation for experiments in animals of the same species (11).

The local ^{14}C concentrations in the tissues are determined by quantitative autoradiography of 20 µm serial sections of frozen brain tissue. Local tissue ^{14}C concentration can be determined from the optical density of the structure in the autoradiograph and a calibration curve relating optical density to concentration obtained from the autoradiographic images of calibrated ^{14}C plastic standards. The procedure of the method is so designed that the autoradiographs reflect mainly the concentrations of [^{14}C] deoxyglucose-6-phosphate in the cerebral tissues; they are, therefore, essentially pictorial representations of the relative rates of local glucose utilization throughout the brain.

Quantitative analysis of the autoradiographs has been greatly facilitated by the application of computerized image-processing techniques (1). The autoradiographs are automatically scanned under computer control, and the optical density of each spot on the film, from 25 to 100 µm as selected, is digitized and stored in the computer. After the plasma [^{14}C] deoxyglucose and glucose concentrations are entered by the operator, the computer converts the optical density of each spot into concentration and then into the local rate of glucose utilization. The autoradiographs are then reconstructed and displayed in color on the face of a color-TV monitor along with a calibrated color scale. The colors represent the rates of glucose

A

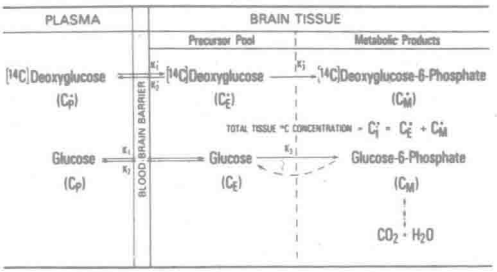

B

Functional Anatomy of the Operational Equation of the [14C] Deoxyglucose Method

General Equation for Measurement of Reaction Rates with Tracers:

$$\text{Rate of Reaction} = \frac{\text{Labeled Product Formed in Interval of Time, 0 to T}}{\left[\text{Isotope Effect Correction Factor}\right]\left[\text{Integrated Specific Activity of Precursor}\right]}$$

Operational Equation of [14C]Deoxyglucose Method:

$$R_i = \frac{\overbrace{C_i^*(T) - k_1^* e^{-(k_2^*+k_3^*)T}\int_0^T C_p^* e^{(k_2^*+k_3^*)t}\,dt}^{\text{Labeled Product Formed in Interval of Time, 0 to T}}}{\underbrace{\left[\frac{\lambda \cdot V_m^* \cdot K_m}{\phi \cdot V_m \cdot K_m^*}\right]}_{\text{Isotope Effect Correction Factor}}\underbrace{\left[\int_0^T \left(\frac{C_p^*}{C_p}\right)dt - e^{-(k_2^*+k_3^*)T}\int_0^T \left(\frac{C_p^*}{C_p}\right)e^{(k_2^*+k_3^*)t}\,dt\right]}_{\text{Integrated Plasma Specific Activity}\;\;\text{Correction for Lag in Tissue Equilibration with Plasma}}}$$

Integrated Precursor Specific Activity in Tissue

Figure 1. (A): Diagrammatic representation of the theoretical model. C_i^* represents the total ^{14}C concentration in a single homogeneous tissue of the brain. C_p^* and C_p represent the concentrations of [^{14}C] deoxyglucose and glucose in the arterial plasma, respectively; C_E^* and C_E represent their respective concentrations in the tissue pools that serve as substrates for hexokinase. C_M^* represents the concentration of [^{14}C] deoxyglucose-6-phosphate in the tissue. The constants k_1^*, k_2^*, and k_3^* represent the rate constants for carrier-mediated transport of [^{14}C] deoxyglucose from plasma to tissue, for carrier-mediated transport back from tissue to plasma, and for phosphorylation by hexokinase, respectively. The constants k_1, k_2, and k_3 are the equivalent rate constants for glucose.

[^{14}C] Deoxyglucose and glucose share and compete for the carrier that transports both between plasma and tissue and for hexokinase which phosphorylates them to their respective hexose-6-phosphates. The dashed arrow represents the possibility of glucose-6-phosphate hydrolysis by glucose-6-phosphatase activity, if any (10,12).

(B): Operational equation of radioactive deoxyglucose method and its functional anatomy. T represents the time at the termination of the experimental period; λ equals the ratio of the distribution space of deoxyglucose in the tissue to that of glucose; ϕ equals the fraction of glucose which, once phosphorylated, continues down the glycolytic pathway; and K_m^* and V_m^* and K_m and V_m represent the familiar Michaelis-Menten kinetic constants of hexokinase for deoxyglucose and glucose, respectively. The other symbols are the same as those defined in Figure 1A (10).

utilization, and the rate of glucose utilization of any 25-100 µm spot in the displayed image of the brain section can be identified from its color. These pictorial displays represent, therefore, color-coded maps of the local rates of glucose utilization throughout the brain.

Rates of local cerebral glucose utilization have been determined quantitatively most frequently in the rat and monkey (Table 1).

The rates in the conscious rat vary widely throughout the brain with values in white matter ranging between 30 and 40 µmoles/100g/min and values in gray matter several fold higher, between approximately 50 and 200 µmoles/100g/min (12). The highest values are found in components of the auditory system with the inferior colliculus clearly the most metabolically active structure in the brain. The rates of glucose utilization in the conscious monkey are similarly distributed, but they are generally one-third to one-half of the values obtained in corresponding regions of the rat brain (5). The differences between the rates in the rat and monkey brains are consistent with the smaller cells more densely packed in the rat brain than in the monkey brain.

The results of numerous studies on the effects of experimentally induced focal alterations of functional activity on local cerebral glucose utilization have demonstrated a close coupling between local functional activity and energy metabolism in the nervous system (9). The effects are often so pronounced that they can be visualized directly in the autoradiographs, or even more so in the color-coded, quantitative, reconstructed maps of cerebral energy metabolism. For example, unilateral electrical stimulation of the sciatic nerve in anesthetized rats increases glucose utilization in the ipsilateral gray matter of the appropriate segments of the spinal cord.

TABLE 1. Representative values for local cerebral glucose utilization in the normal conscious albino rat and monkey (μmoles/100g/min)

Structure	* Albino Rat(10)	+ Monkey(7)
	Gray Matter	
Visual Cortex	107 ± 6	59 ± 2
Auditory Cortex	162 ± 5	79 ± 4
Parietal Cortex	112 ± 5	47 ± 4
Sensory-Motor Cortex	120 ± 5	44 ± 3
Thalamus: Lateral Nucleus	116 ± 5	54 ± 2
Thalamus: Ventral Nucleus	109 ± 5	43 ± 2
Medial Geniculate Body	131 ± 5	65 ± 3
Lateral Geniculate Body	96 ± 5	39 ± 1
Hypothalamus	54 ± 2	25 ± 1
Mamillary Body	121 ± 5	57 ± 3
Hippocampus	79 ± 3	39 ± 2
Amygdala	52 ± 2	25 ± 2
Caudate-Putamen	110 ± 4	52 ± 3
Nucleus Accumbens	82 ± 3	36 ± 2
Globus-Pallidus	58 ± 2	26 ± 2
Substantia Nigra	58 ± 3	29 ± 2
Vestibular Nucleus	128 ± 5	66 ± 3
Cochlear Nucleus	113 ± 7	51 ± 3
Superior Olivary Nucleus	133 ± 7	63 ± 4
Inferior Colliculus	197 ±10	103 ± 6
Superior Colliculus	95 ± 5	55 ± 4
Pontine Gray Matter	62 ± 3	28 ± 1
Cerebellar Cortex	57 ± 2	31 ± 2
Cerebellar Nuclei	100 ± 4	45 ± 2
	White Matter	
Corpus Callosum	40 ± 2	11 ± 1
Internal Capsule	33 ± 2	13 ± 1
Cerebellar White Matter	37 ± 2	12 ± 1

The values are the means ± standard errors from measurements made in the number of animals indicated in parentheses.
* Sokoloff et al. (12)
+ Kennedy et al. (5).

Focal seizures induced by injection of penicillin into the motor cortex of one side of the monkey brain elicit increased glucose utilization in discrete regions of the ipsilateral motor cortex, putamen, globus pallidus, thalamic nuclei, substantia nigra, etc. Bilateral obstruction of the auditory canals in conscious rats markedly diminishes glucose utilization bilaterally in all components of the auditory system; with unilateral obstruction some structures are affected only ipsilaterally, some bilaterally, and some only contralaterally; with quantification it